SUPPORTING INFORMATION

Non-thermal Magnetic Deicing Using Two-Dimensional Chromium Telluride

Chinmayee Chowde Gowda[1], *Alexey Kartsev*[2,3,4*], *Nishant Tiwari*[5], *Safronov A.A*[3], *Prafull Pandey*[6], *Ajit K. Roy*[7], *Pulickel M. Ajayan*[8], *Douglas S. Galvão*[9*] *and Chandra Sekhar Tiwary*[1,5]

[1]School of Nano Science and Technology, Indian Institute of Technology Kharagpur, West Bengal – 721302, India

[2]Computing Center of the Far Eastern Branch of the Russian Academy of Sciences, 680000 Khabarovsk, Russia

[3]MIREA-Russian Technological University, 119454 Moscow, Russia

[4]Peoples' Friendship University of Russia (RUDN University), 6 Miklukho-Maklaya St, Moscow 117198, Russia

[5]Department of Metallurgical and Materials Engineering, Indian Institute of Technology Kharagpur, West Bengal – 721302, India

[6]Materials Engineering, Indian Institute of Technology Gandhinagar, Gujurat – 382055, India

[7]Materials and Manufacturing Directorate, Air Force Research Laboratory, Wright Patterson AFB, Ohio, 45433-7718, USA

[8]Department of Materials Science and NanoEngineering, Rice University, 6100 S Main Street, Houston, TX 77005, USA

[9] Applied Physics Department and Computational Engineering and Sciences, State University of Campinas, Campinas, SP, 13083-970, Brazil

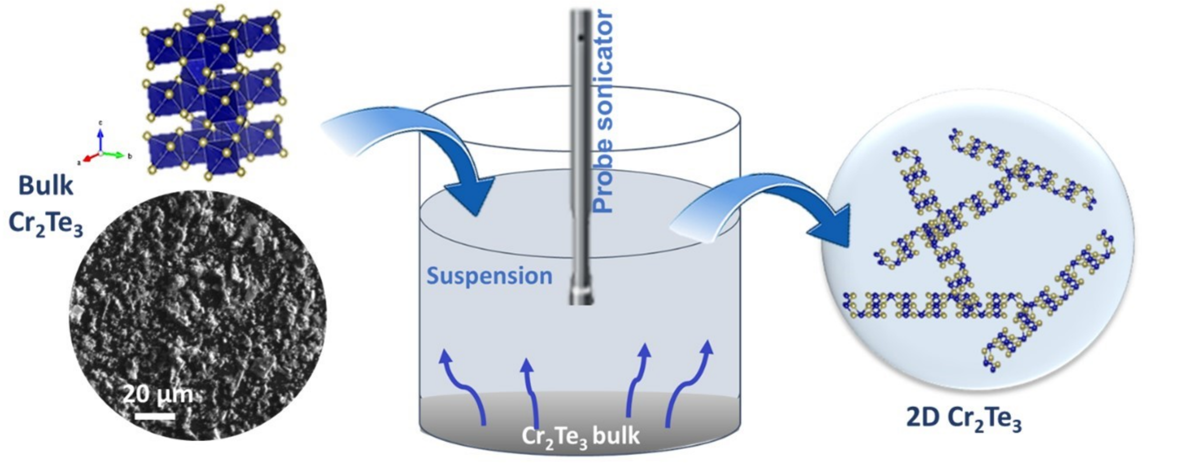

Figure S1: *Schematic representation of the liquid phase exfoliation technique (inset down: SEM image of bulk Cr_2Te_3 crushed sample).*

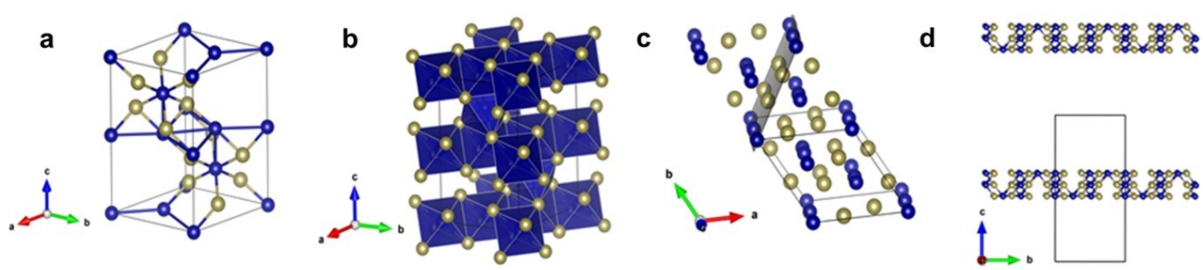

Figure S2: *Volumetric view of the original structure, (a) Cr atoms are shown in blue, Te atoms in yellow, (b) volumetric view of the original structure in the polyhedron model, (c) plane $(11\overline{0})$ in the original structure and (d) initial 2D structure.*

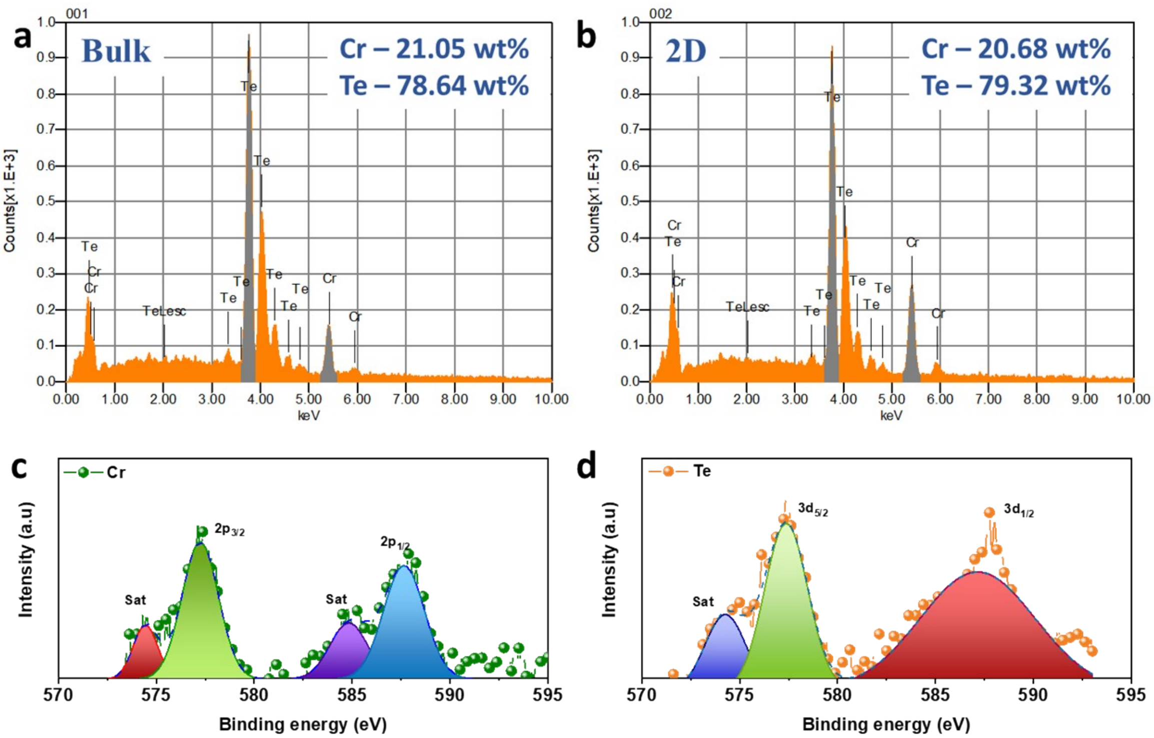

Figure S3: *Elemental analysis of (a) bulk sample after homogenization, and (b) 2D* Cr_2Te_3*, (c) XPS survey spectra of* Cr_2Te_3 *(c) Chromium and (d) Tellurium.*

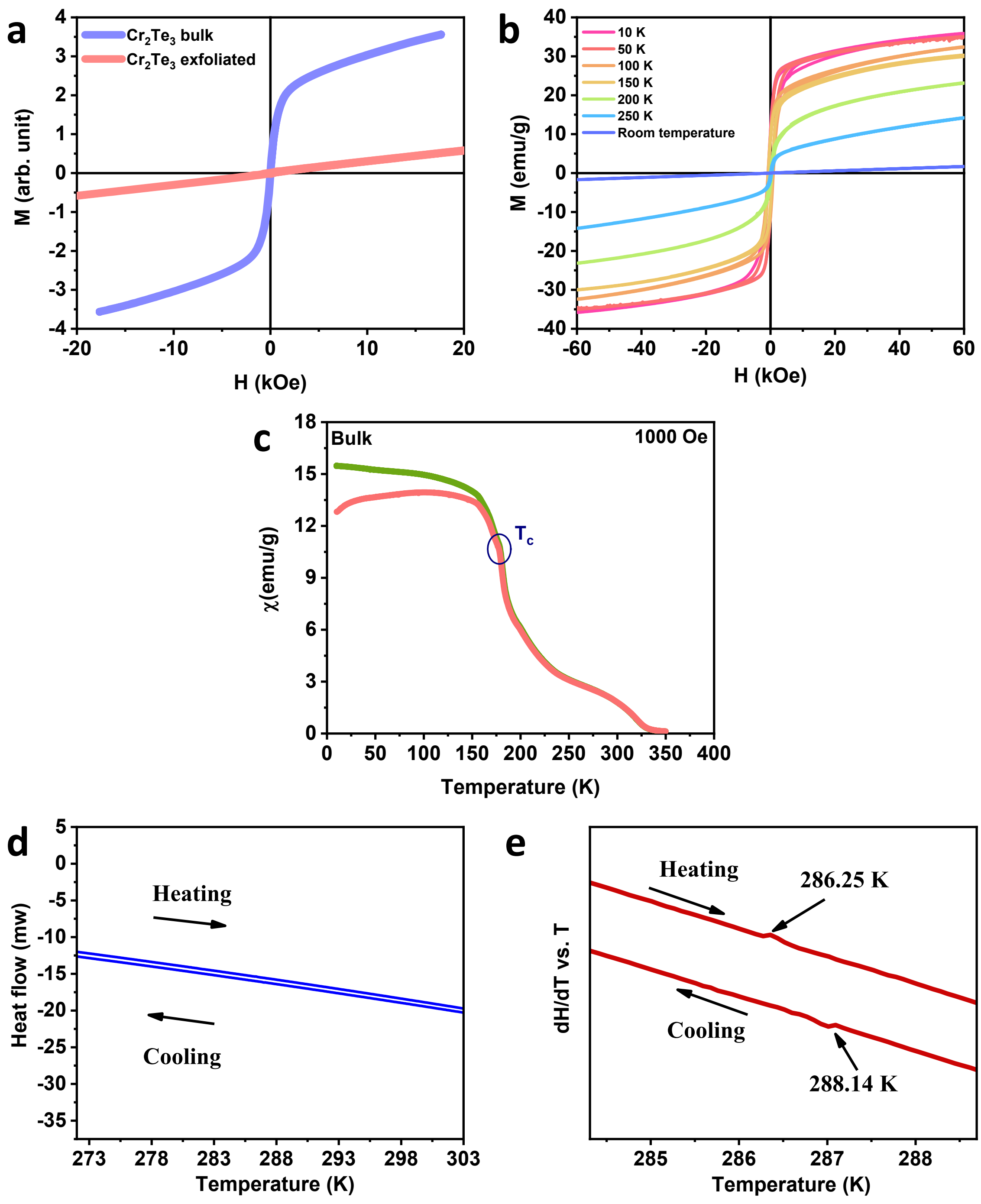

Figure S4: *Magnetic behavioural studies (a) M-H loop of bulk and 2D Cr_2Te_3 at room temperature, (b) M-H loop at temperatures ranging from 10 K to 300 K (50 K intervals) and (c) FC-ZFC curves depicting T_C at 180 K for bulk Cr_2Te_3 (d) DSC data showing heating and cooling curves and (e) dH/dT vs. T curves.*

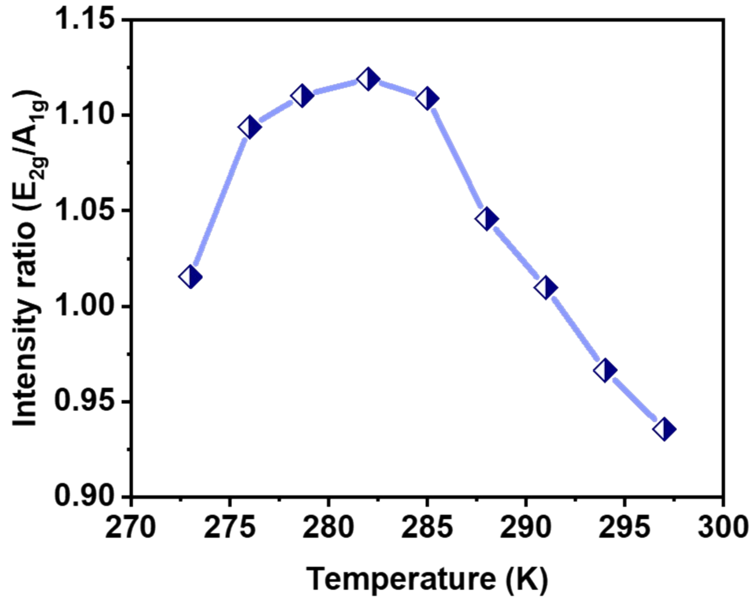

Figure S5: *Intensity ratio shift of two major Raman bands during heating conditions (273 K to 297 K).*

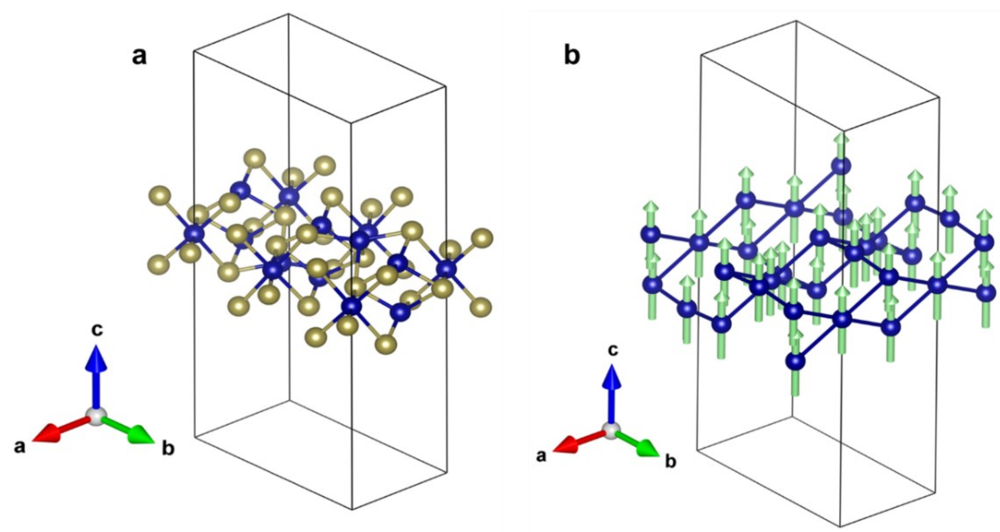

Figure S6: *(a) Final view of the 2D structure Cr_2Te_3 and (b) magnetic sublattice Cr.*

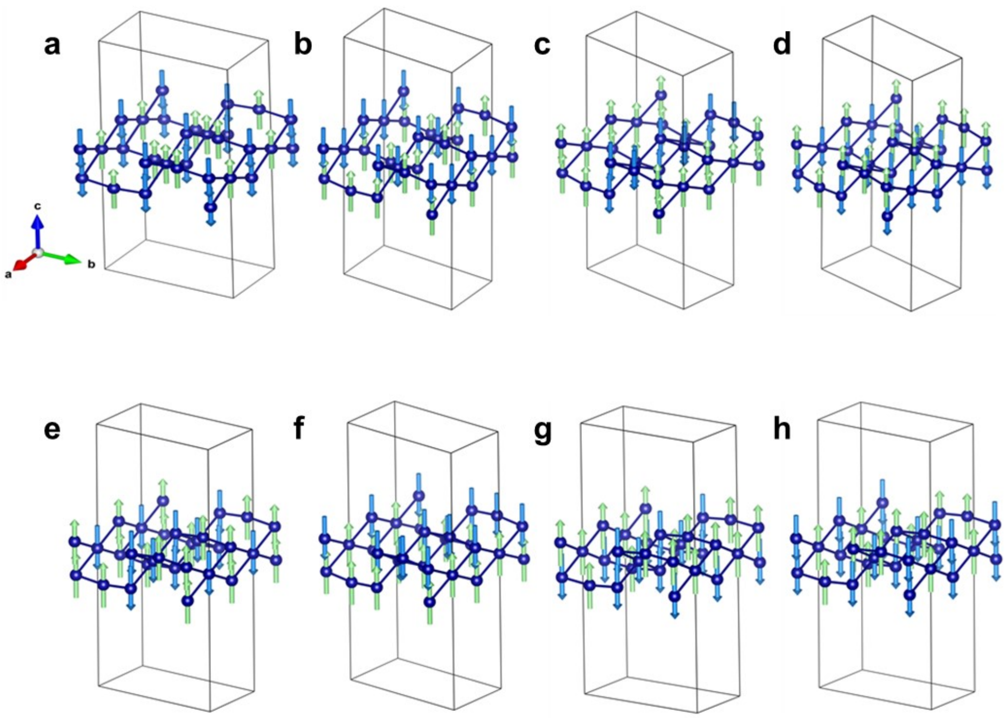

Figure S7: *Magnetic sublattice Cr of the final system with possible orientations of the spin magnetic moment in the antiferromagnetic structure (a-h).*

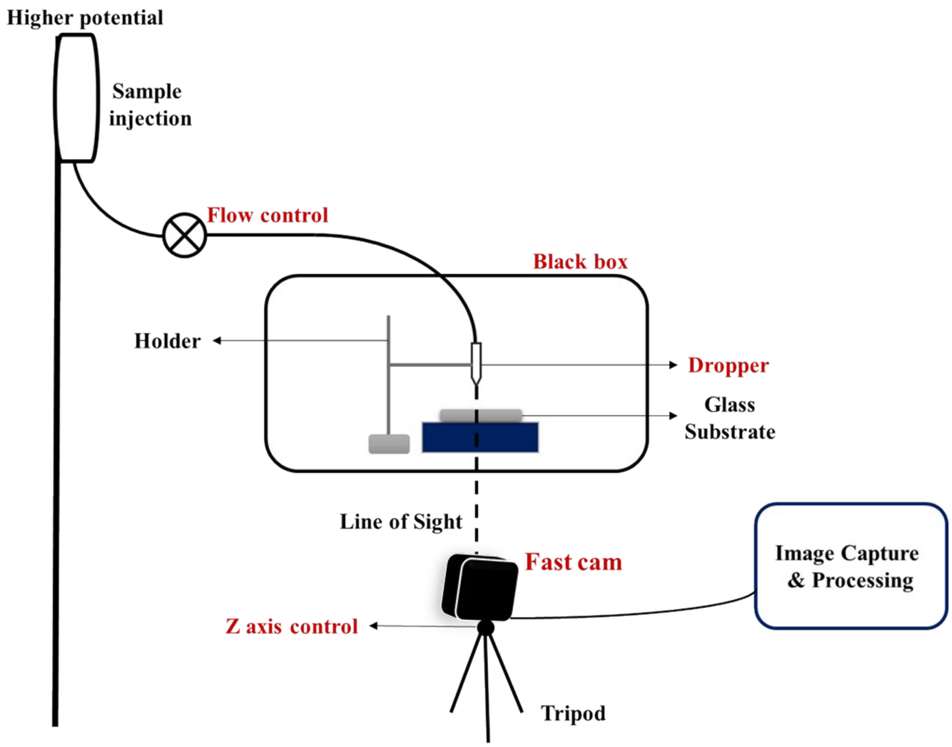

Figure S8: *Schematic diagram of 2D Cr_2Te_3 drop on glass substrate for wettability study.*

High speed camera specifications:

Model: Fastcam Mini UX 50 type 160 K – M – 4G

Frame rate: 2000 fps

Shutter speed: 1/ frame sec

Resolution: 1280 x 1024

Frame count: 2180 frame

Rec duration: 1.09 sec

Trigger mode: Start

Zoom ratio: 422 % (Variable)

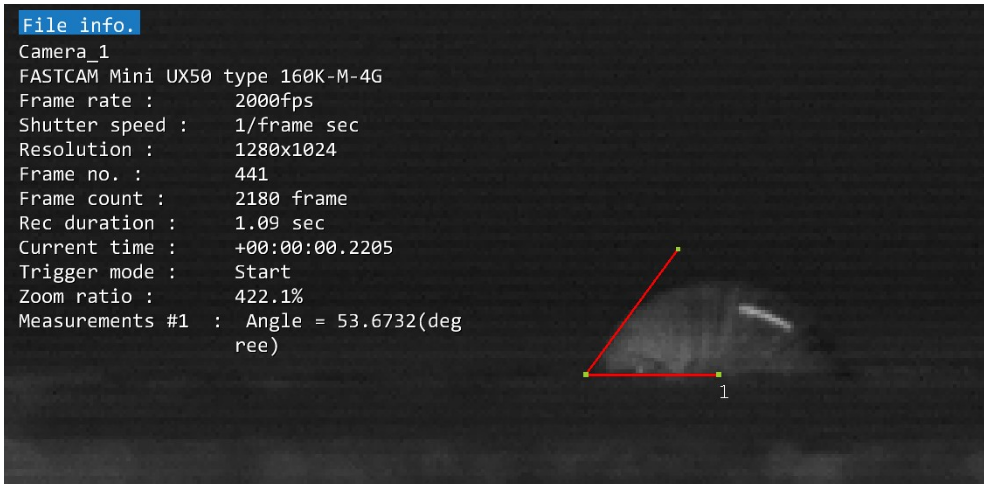

Figure S9: *Single frame captured during measurement of water contact angle (Bulk Cr_2Te_3 in this case) from Photron photo viewer software (PFV4 (×64)).*

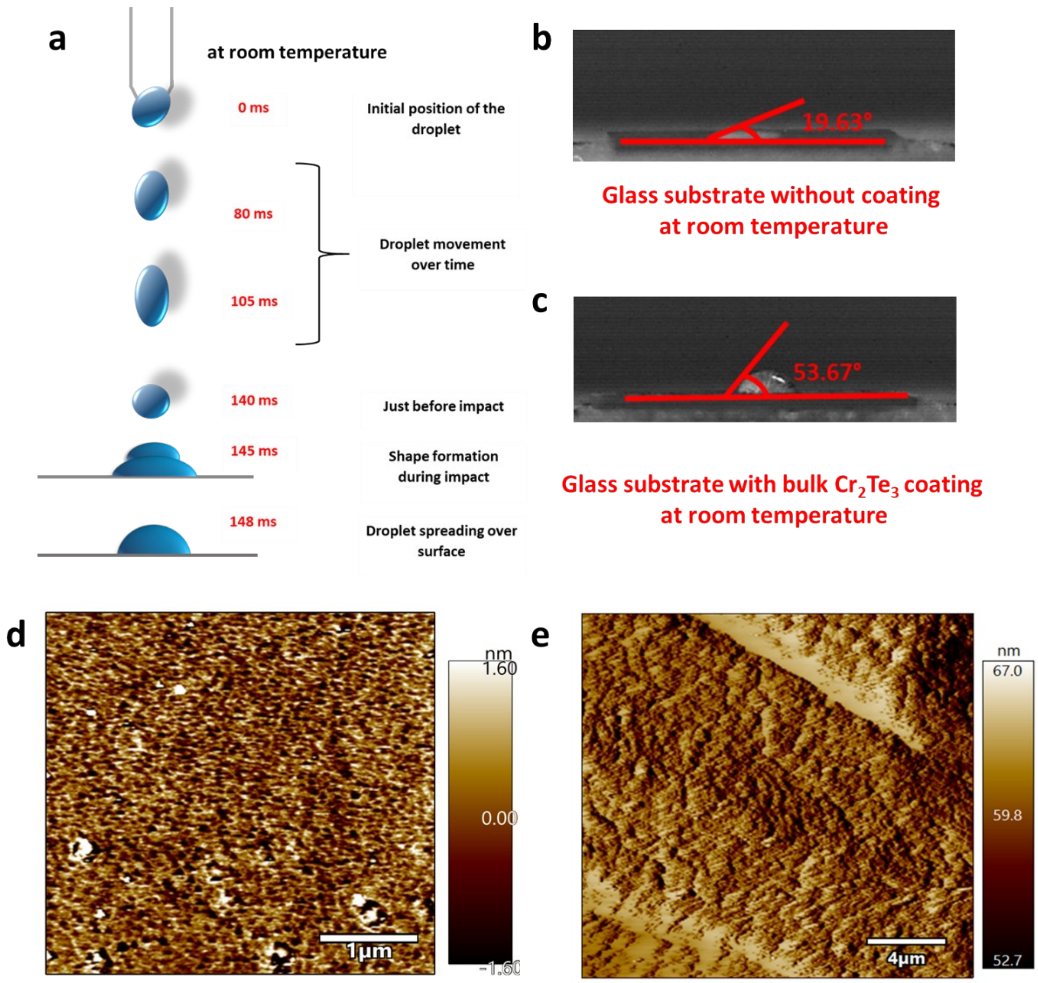

Figure S10: *(a) Schematic representation of water drop falling on a surface, Contact angle measurement on (b) plane glass substrate and (c) bulk Cr_2Te_3 coating, Surface morphology obtained by AFM (d) 2D Cr_2Te_3 and (e) Bulk Cr_2Te_3.*

Surface Interaction studies:

We have considered two cases of ice attachment to chromium telluride (**Figure S11**). The formation energy E^{form} of the 1L-H_2O/Cr_2Te_3 structure was calculated as follows:

$$E^{form} = E^{tot}(1L - H_2O/Cr_2Te_3) - E^{tot}(1L - H_2O) - E^{tot}(1L - Cr_2Te_3) \qquad (S1)$$

where, $E^{tot}(1L\text{-}H_2O/Cr_2Te_3)$, $E^{tot}(1L\text{-}H_2O)$ and $E^{tot}(1L\text{-}Cr_2Te_3)$ are the total energies of 1L-H_2O/Cr_2Te_3 structure, ice crystal monolayer and 1L-Cr_2Te_3 monolayer, respectively. The obtained vdW gap values between the Cr_2Te_3 and H_2O layers are 1.9 and 2.3 Å for the ferromagnetic and paramagnetic structure, respectively. The formation energies of different combinations are tabulated in **Table S1**.

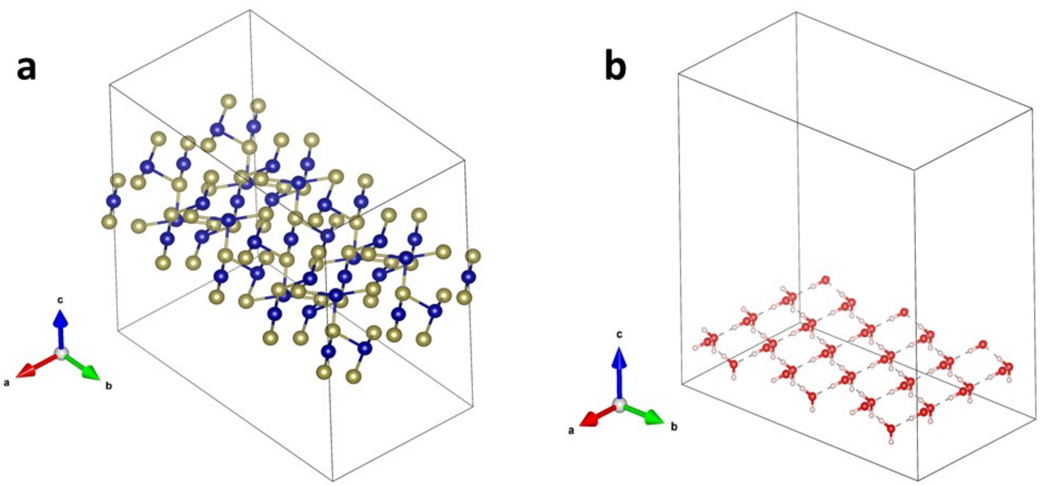

Figure S11: *(a) 1L-Cr_2Te_3 2×2 supercell and (b) 1L-H_2O 3×3 supercell*

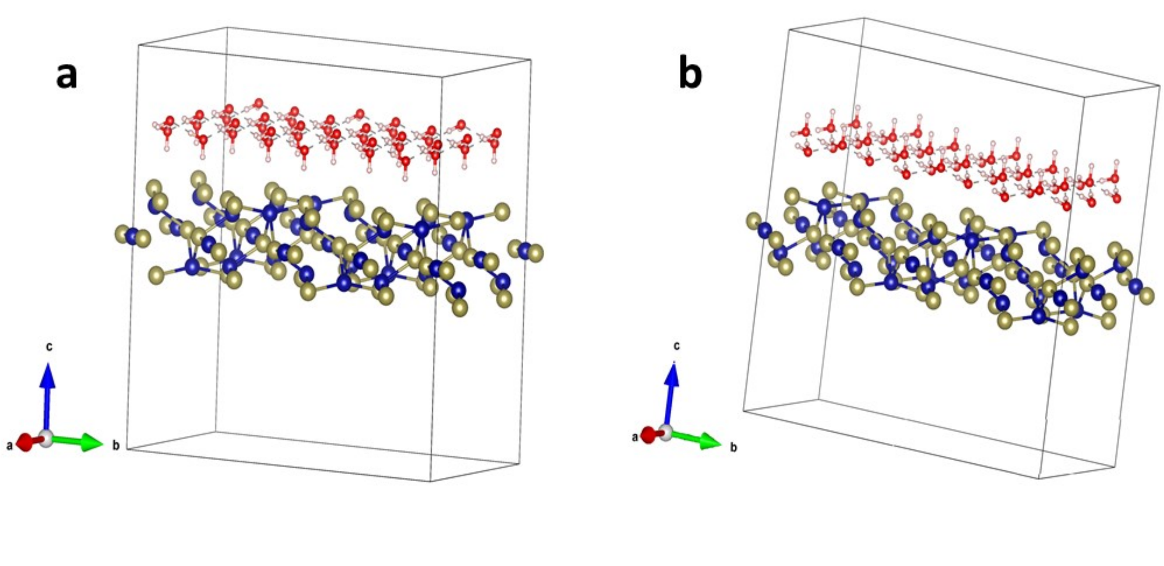

Figure S12: *Two cases of ice attachment to chromium telluride. (a) Oxygen ions oriented towards the chromium telluride plane (O-oriented), (b) hydrogen ions oriented towards the chromium telluride plane (H-oriented).*

Table S1. *Structural parameters (α = 90°, β = 90°) and calculated formation energy E^{form} for relaxed 1L-H_2O/Cr_2Te_3 heterostructures in four variants.*

Structure	**a, b (Å)**	**E^{form} (eV/H_2O)**
1L-H_2O/Cr_2Te_3 FM Cr_2Te_3 O-faced toward H_2O	a=12.72 b=23.49	0.242
1L-H_2O/Cr_2Te_3 FM Cr_2Te_3 H-faced toward H_2O	a=12.73 b=23.31	0.258
1L-H_2O/Cr_2Te_3 PM Cr_2Te_3 O-faced toward H_2O	a=12.57 b=23.29	0.390
1L-H_2O/Cr_2Te_3 PM Cr_2Te_3 H-faced toward H_2O	a=12.59 b=23.33	0.385

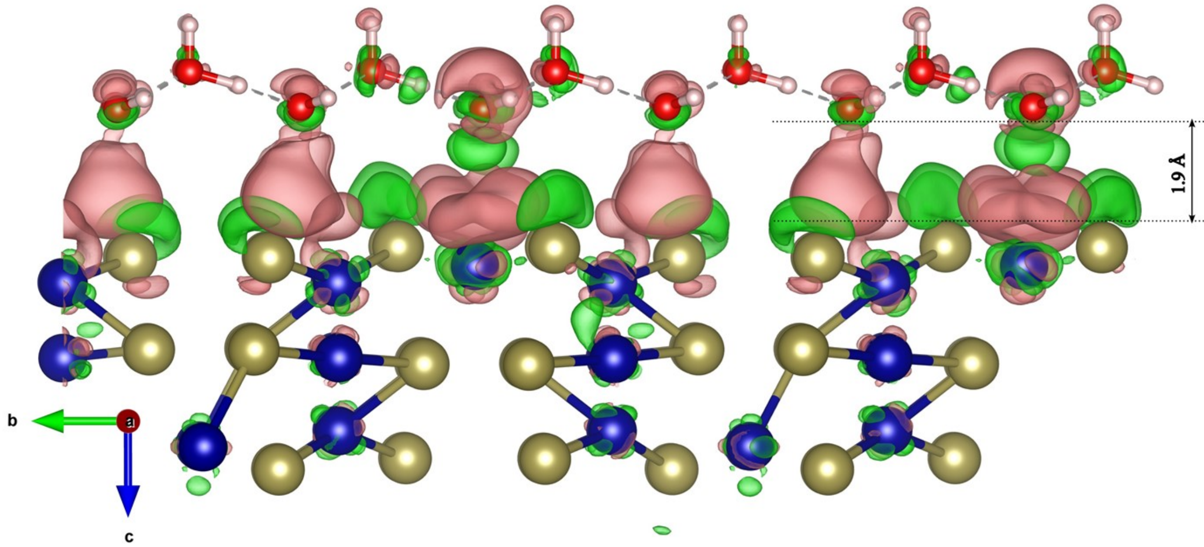

Figure S13: *Charge transfer isosurface (3·10^-4 e/Å) between ice and ferromagnetic* Cr_2Te_3 *monolayers. Red/green color correspond to the negative/positive charge difference. Dashed lines indicates the vdW gap between ice and substrate.*

The charge transfer were computed using the following formalism:

$$\Delta\rho = \rho^{Cr_2Te_3/H_2O} - \rho^{1Ltext-Cr_2Te_3} - \rho^{1Ltext-H_2O} \tag{S2}$$

where $\rho^{Cr_2Te_3/H_2O}$ is the charge density for the ice/Cr_2Te_3 total monolayered structure, $\rho^{1Ltext-Cr_2Te_3}$ and $\rho^{1Ltext-H_2O}$ are charge density for the bare Cr_2Te_3 and bare H_2O monolayers, respectively. The charge transfer isosurface between ice and FM Cr_2Te_3 ML was 3×10^{-4} e/ Å.

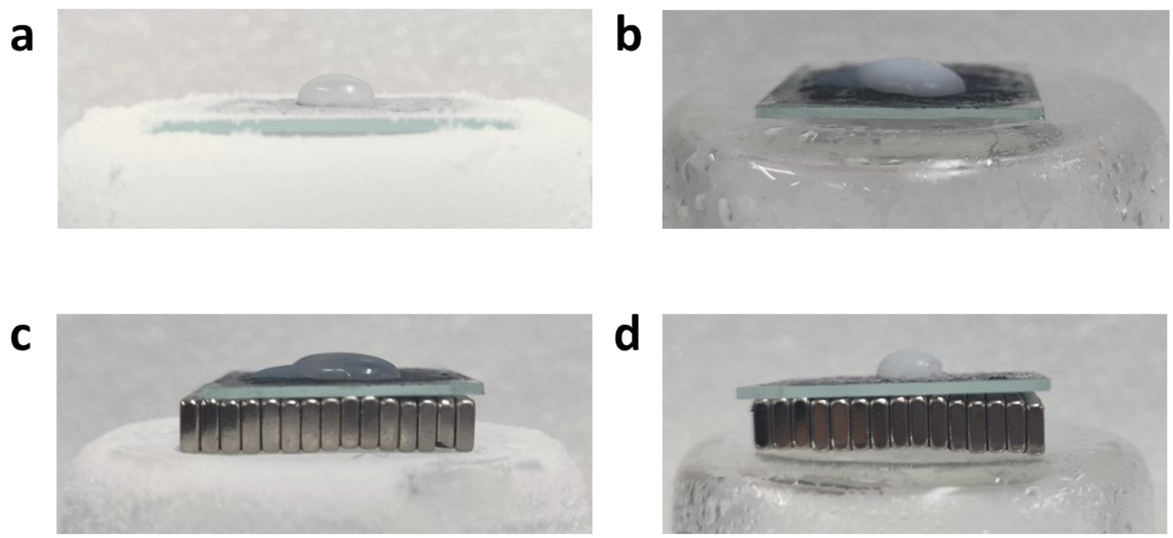

Figure S14: *(a) Oil droplet on bare frozen surface (without magnetic field) at 0°C and (b) at Room temperature (> 25 °C), (c) Oil droplet on application of external magnetic field at 0°C and (d) at Room temperature (> 25 °C).*